

Improved Binary Artificial Fish Swarm Algorithm for Diagnosis of Thyroid Disease

Suryaa Pranav Meduri

Lambton College, Mississauga, ON, Canada

Meduri Anupama

*Department of CSE, Maturi Venkata Subba Rao (MVSR)
Engineering College, Hyderabad, India*

Abstract: The thyroid gland generates the thyroid hormones, which help the appropriate body's metabolism regulation. Generally, the abnormalities of thyroid function are categorized into two classifications such as small thyroid hormone production called hypothyroidism or large thyroid hormone production named hyperthyroidism. The thyroid diagnosis using suitable thyroid data interpretation is considered a very important classification problem. Till now, few contributions are performed in the automatic diagnosis of thyroid disease. The main aim of this research is to work on a novel diagnosis of thyroid approach, which follows a new working model. Here, it dealt with the integration of both the thyroid data and image. Moreover, two important working procedures are carried out such as classification as well as feature extraction. In the initial stage, two feature sorts are extracted. Image features such as gradient as well as neighborhood-based features are extracted and the principle component analysis (PCA) process is included for the feature extraction from thyroid data. Then, the process of classification is carried out in two segments. Here, the Convolutional Neural Network (CNN) is exploited to obtain the classified outcomes bypassing the image itself. At the same time, in order to obtain the data features and image as the input, the Neural Network (NN) is exploited for the classification procedure. At last, both the classified outcomes such as NN as well as CNN are integrated to raise the precise diagnosis rate. Furthermore, the main contribution of this paper is to raise the rate of accuracy, therefore this work attempts to activate the optimization model. In CNN, the convolution layer is optimally chosen and when classifying in the NN model the subjected feature must be optimal. Therefore, the necessary features are chosen optimally. For this purpose, a novel enhanced approach called Improved Binary Artificial Fish Swarm Algorithm (IBASFS) is the enhancement model of Fish Swarm Algorithm is presented in this paper. At last, the adopted model performances are evaluated with the existing models and it reveals that the enhancement of the adopted model to detect the thyroid.

Keywords: Classification, Data, Neural Network, Image, Thyroid Hormone.

Nomenclature

Abbreviations	Descriptions
CT	Computerized Tomography
SVM	Support Vector Machines
US	Ultrasound
NSWs	Night Shift Workers
CBIR	Content-Based Image Retrieval
LDA	Linear Discriminant Analysis
BOW	Bag of visual Words
TSH	Thyroid Stimulating Hormone
CAD	Computer-Aided Diagnosis
TFT	Thyroid Function Test
KNN	k-nearest neighbor
VEGFR	Vascular Endothelial Growth Factor Receptor
FNA	Fine Needle Aspiration
GA	Genetic Algorithm
RCC	Renal Cell Carcinoma
HR	Hazard Ratio

1. Introduction

Thyroid disease can be affected by the people in wide-reaching, subsequent to affect the people's turns out to be a severe health issue. The thyroid gland is considered one of the significant organ of the human

body. It generates the thyroid hormone that is fundamental to control the body's metabolism. Thyroxine and triiodothyronine are two active thyroid hormones that encompass significant effects on the production of protein, production of energy, regulation of body temperature, and human body energy regulation. Hence, the metabolism and human body regulation will lose essential control and which might be life-threatening in severe cases if the thyroid gland is diseased [1].

In diagnosing thyroid disease, these hormones play a significant role, as thyroid hormones are necessary for brain normal growth as well as neural system, particularly in the primary three years of life and in the event of their malfunction, mental retardation may happen. In senior ages, children to have suitable growth, and adults to have a usual metabolism and regulating their body mechanism, require thyroid hormones. For this reason, at the primary instant of birth, a thyroid regulation test is performed on babies in a few countries. Generally, thyroid diseases are amid women than men. In thyroid disease, significant factors are hypothyroidism, hyperthyroidism, autoimmune disorders, thyroid inflammation, as well as thyroid cancer [2].

To diagnose thyroid diseases, the CT, as well as the US, is a well-liked imaging modality. US imaging is non-invasive, reasonably priced, and simple to utilize [3]. US images are frequently developed because of their cost-effectiveness and portability in smaller hospitals. The thyroid is compatible with ultrasound research owing to its outward position, size as well as echogenicity. For Thyroid Ultrasound, the CAD is essential to delineate the nodules, classify malignant/benign as well as estimate the thyroid tissues volumes to augment reliability and minimize invasive operations like FNA as well as a biopsy [4].

Experimentation of the human visual model, computer vision is with the benefits of minimum cost as well as maximum detection speed. Computer vision application is frequently exploited in the field of speedy intelligent image processing, like object detection, image classification, as well as to object retrieval. In the previous phase of computer vision, many studies had concentrated on modeling the feature indications for CBIR five tens of years [5].

The objectives involved global features like shape, color, and texture; local features like SIFT and SURF features; as well as BOW representations. Subsequently, Machine Learning techniques like KNN, SVM, and LDA were extensively exploited in image classification. The SIFT technique is exploited to extract the image to recognize prostate cancer. Several new techniques, like fuzzy classifiers, pattern recognition methods, artificial immune recognition systems, NN, neuro-fuzzy, GA so on, were exploited for thyroid disease diagnosis.

The main aim of this paper is to present a novel thyroid diagnosis model which integrates both the extraction of features as well as the classification model. Here, two kinds of input are subjected such as data as well as image. In the feature extraction phase, both the data as well as image features are extracted. Moreover, to extract the data features the PCA process is exploited. In the classification stage, two sorts of classification are carried out. Here, CNN is employed to classify the image as well as NN is employed in the classification procedure by attaining the extracted features as the input. The optimal features are chosen using the novel optimization approach. Likewise, the optimal convolutional layer is chosen using the IBASFS algorithm, and these optimal selections are merely used to increase the diagnosis accuracy rate.

2. Literature Review

In 2012, Yen-Chung Lin et al [1], explained the clinical effect of abnormal thyroid function in enduring PD patients. This paper was the case-controlled demonstration as well as a longitudinal research. Here, they had gathered laboratory data, indications, and parameters of dialysis and thyroid and patient heart function. An aforesaid subject elucidated a new account of infection or took any drugs or inflammatory disease called as the weight thyroid function. Abnormal thyroid function was explained as the most important hypothyroidism presence as well as the sick euthyroid syndrome. In 2008, I. Tamaskar et al [2], worked on the Sorafenib, which was an orally bioavailable VEGFR inhibitor by means of the antitumor activity in metastatic RCC. In addition, the Sunitinib which was a VEGFR inhibitor persuades biochemical hypothyroidism in 85% of metastatic RCC patients, the mainstream of who have signs of hypothyroidism symptoms. Therefore, the TFT occurrence abnormalities in patients by means of metastatic RCC attaining sorafenib were examined. In 2019, G. Singh et al [3] predicted the abnormal TSH in transfusion-dependent thalassemia. Between 90 children with transfusion-dependent thalassemia registered in the Division of Pediatric Hematology-Oncology, 43 children 6-18 years of age on regular blood transfusion they undergo thyroid function test as part of our unit protocol were enrolled for the examination". Patients were categorized into two classifications that is TSH >5.5 mIU/L, as well as TSH ≤ 5.5 mIU/L, which were evaluated regarding gender, age, as well as serum ferritin. In 2021, Hsin-Hao Chen et al [4] worked on abnormal TSH and the examination was carried in NSWs and they exhibited a high risk of abnormal TSH. A study was carried out for 574 employees, which was based on the retrospective cohort and it was performed for abnormal TSH as well as without thyroid disease at baseline. The rate of incidence was calculated as well as the adjusted HR was estimated for subclinical

hypothyroidism as well as incident abnormal TSH was evaluated with non-NSWs by exploiting a Cox regression technique. Sabath, E et al [5], worked on the thyroid function tests which were obtained from January 2017 to September 2019 were examined from the Core Laboratory of the State Health Services that was the referral center for all the hospitals of the State and serving a total population of 1,176,000 inhabitants.

3. Diagnosis of Thyroid Model

3.1 Description of the proposed model

The complete idea of the presented diagnosis technique is described in this section. This paper introduces the novel criterion by combining both the data and the thyroid image as input. Here, two stages are introduced such as feature extraction as well as classification. At the initial stage, two sets of features are extracted, from the input image, the image features such as gradient as well as neighborhood based features are extracted as well as to extract the features the PCA process is used from data input. In the subsequent stage, that is the classification stage two sort of classification is carried out. Here, the CNN model is exploited to classify the image directly. Then, to diagnose the thyroid the NN is exploited by obtaining the data as well as image features. To obtain the classification outcome, both the classification results are integrated together. In addition, the adopted technique tries to create a high level of the objective to find the optimal solutions. To raise the diagnosis accuracy, two important contributions are carried out in the classification stage. The CNN convolutional layer is optimally chosen therefore the CNN classification turns out to be highly accurate. Furthermore, the features which are subjected as the input to the NN are optimally chosen thus raising the rate of accuracy. This work develops a novel optimization approach to identify the optimal solutions. Fig 1 demonstrates the block diagram of the adopted diagnosis model.

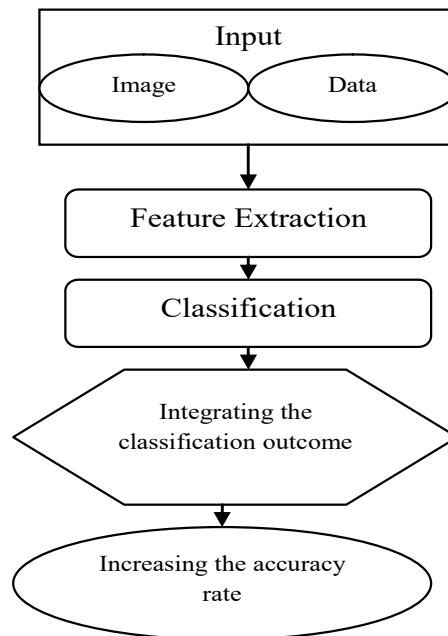


Fig. 1. Block diagram of adopted Diagnosis model

4. Feature Extraction in Adopted Diagnosis Model

Two sorts of feature extraction are carried out in this section that is the gradient as well as neighbourhood-based feature from an image as well as the data extraction feature is performed by exploiting the process of PCA.

4.1 Image features

In this stage, the features such as “neighborhood based and gradient features are extracted from the image and the LVP” are attained. The LVP process [6] is as stated as below:

The local sub-region R is subjected from the given input image, as well as $VE_{\beta,DI}(P_c)$ indicates the vectors' direct value. Moreover, DI represents the distance between the referenced pixel and its neighboring pixels with β direction, β indicating in different direction's index angles. Eq. (1) indicates the value of vector's direction as P_c it represents the referenced pixel.

$$VE_{\beta,DI}(P_c) = (R(P_{\beta,DI}) - R(P_c)) \quad (1)$$

The $LVP_{PA,RE,\beta}(P_c)$ LVP pattern at P_c is encoded in β direction of the vector. At last, eq. (2) states the $LVP_{PA,RE}(P_c)$ LVP pattern at P_c is ascertained as the concatenation of the 4 8-bit binary patterns LVPs.

$$LVP_{PA,RE}(P_c) = \{LVP_{PA,RE,\beta}(P_c) | \beta = 0^\circ, 45^\circ, 90^\circ, 135^\circ\} \quad (2)$$

In addition, for the gradient feature, the LVP patterns are extracted. From the image, to extract the information, the image gradients are used. From the original image, the gradient images are produced and each gradient image pixel measures the intensity change of that same point in the original image. In both x and y directions gradient images are calculated to obtain the complete range of direction. In addition, the image gradient is a vector of its partials.

$$\nabla_f = \begin{bmatrix} gr_x \\ gr_y \end{bmatrix} = \begin{bmatrix} \frac{\partial f}{\partial x} \\ \frac{\partial f}{\partial y} \end{bmatrix} \quad (3)$$

In Eq. (3), $\frac{\partial f}{\partial x}$ denote derivative regarding x as well as $\frac{\partial f}{\partial y}$ denote derivative regarding y .

4.2 Data features using PCA

PCA [8] is used for the extraction of data features. At first, the eigenvectors recognition of the correlation matrix is performed as well as the eigenvectors with superior eigenvalues are worried. It is stated as the I input vectors transformation with a similar length H in I -dimensional vector $a = [a_1, a_2, \dots, a_I]^T$ into a vector b as stated as Eq. (4).

$$b = A(a - me_a) \quad (4)$$

Each a row involves H values. In Eq. (4), me_a vector denotes mean vector that is mathematically stated in Eq. (5).

$$me_a = M\{a\} = \frac{1}{H} \sum_h a_h \quad (5)$$

In Eq. (4), A matrix is stated from the covariance matrix CM_a . Row in A a matrix comprises eigenvectors of CM_a that is arranged based on the corresponding Eigenvalues in downward order. As in Eq. (6), CM_a attainment is by the relation, a is I -dimensional and covariance matrix size is $I \times I$. As per eq. (7), the covariance between $a_1, a_{1'}$ is stated and the number of modules to retain is described using the relation, and it is stated in Eq. (8), wherein, H indicates the number of retained principal components, VA indicates the Eigenvalues, NU indicates the total number of Eigenvalues.

$$CM_a = M\{a - me_a)(a - me_a)^T\} = \frac{1}{H} \sum_{h=1}^H a_h a_h^T - me_a me_a^T \quad (6)$$

$$CM_a(1, 1') = M\{(a_1 - me_1)(a_{1'} - me_{1'})\} \quad (7)$$

$$\frac{\sum_{l=1}^{NU} VA_l}{\sum_{h=1}^H VA_h} = \alpha \quad \text{where } 0 < \alpha \leq 1 \quad (8)$$

At last, the attained image and features of data are represented as FE_1, FE_2, \dots, FE_N .

5 Classification Procedure using Adopted Case

The process of classification is described in this section. Here, two sorts of classifications are carried out. At first, by exploiting the CNN approach the image classification is performed as well as the NN models are exploited to classify the image by subjecting the data features as input.

5.1 CNN Model

Generally, CNN [7] is primarily modeled to deal with the variability of 2D shapes. The technique is clearly modeled to extract the image features. Mostly, the CNN involves two layers as a) Convolutional layer, b)

Pooling layer. In addition, the CNN integrates multiple phases besides the classification phase. Both the input and output of the layer are considered by the feature maps. The feature map size is minimized layer by layer using the CNN propagation as well as features are extracted are actually intangible and worldwide.

The image patches indication is like $i_0 = \{i_1, i_2, \dots, i_S\}$, wherein S indicates the number of training samples. Via the patch extraction centered on $p = \{p_1, p_2, \dots, p_N\}$, these samples are obtained. The relevant network output is indicated as $j = \{j_1, j_2, \dots, j_S\}$ for $i_0 = \{i_1, i_2, \dots, i_S\}$. Each j_s gets the value from the ascertained set of classes $\Omega_1 = \{1, 2, \dots, C\}$, wherein le signifies network level, C signifies a number of classes that obtains the value from the level set, $\Omega_1 = \{1, 2, \dots, LE\}$.

Here, eq. (9) indicates the performance of the CL, which acts as the previous layer output convolution beside the sliding filter bank to generate the feature map of the output. Moreover, i_n^{le-1} signifies n^{th} input feature map in $(le-1)$ layer, G_k^{le} signifies k^{th} output feature map in le layer, $\text{sig}(\cdot)$ and signifies sigmoid function that is used for the activation function of network's. Both w_{kn}^{le} and d_k^{le} indicates the filters which comprise the convolutional layers' training parameters.

$$G_k^{le} = \text{sig} \left(\sum_{n=1}^m i_n^{le-1} * w_{kn}^{le} + d_k^{le} \right) \quad (9)$$

The pooling layer reduces the resolution of the feature map as well as reduces the output sensitivity. Generally, max pooling is exploited as pooling in CNN and it is shown in eq. (10).

$$\begin{aligned} K_k^{le} &= \max\{in_1, in_2, in_3, in_4\} \\ in_1 &= i_n^{le-1} (1 : r : \text{size}(i_n^{le-1}, 1), 1 : r : \text{size}(i_n^{le-1}, 2)) \\ in_2 &= i_n^{le-1} (1 : r : \text{size}(i_n^{le-1}, 1), 2 : r : \text{size}(i_n^{le-1}, 2)) \\ in_3 &= i_n^{le-1} (2 : r : \text{size}(i_n^{le-1}, 1), 1 : r : \text{size}(i_n^{le-1}, 2)) \\ in_4 &= i_n^{le-1} (2 : r : \text{size}(i_n^{le-1}, 1), 2 : r : \text{size}(i_n^{le-1}, 2)) \end{aligned} \quad (10)$$

Here, K_k^{le} indicates the k^{th} output feature map of the pooling layer. Furthermore, the primary and secondary dimensional sizes of i_n^{le-1} are represented as $\text{size}(i_n^{le-1}, 1)$ and $\text{size}(i_n^{le-1}, 2)$, correspondingly. The pooling layer is the entirely linked layer pursued by the convolutional layer. The feature map which subjected as the output and it is transformed into i^{le-1} vector where di denotes vector dimension. Eq. (11) explains the output of full connected layers, wherein, i_n^{le-1} represents n^{th} element in i^{le-1} , O_k^{le} represents k^{th} full connected layer output unit. d_k^{le} bias, as well as filter, are ascertained as the full connected layer trainable parameter.

$$O_k^{le} = \text{sig} \left(\sum_{n=1}^d i_n^{le-1} \times w_{kn}^{le} + d_k^{le} \right) \quad (11)$$

Finally, the formulation of output is stated in eq. (12), and it is in the structure of softmax units, wherein O_s represents feature vector which is derived from the fully connected layer, j_s represents actual output, and θ indicates the softmax function parameter.

$$o(j_s = k | O_s; \theta) = \frac{e^{\theta_k^T O_s}}{\sum_{k=1}^C e^{\theta_k^T O_s}} \quad (12)$$

The process of forward propagation such as softmax classifier convolutional layer, pooling layer, as well as fully connected layer. By exploiting the BPP, the parameters are trained and loss function is determined in Eq. (13).

$$L(\theta) = -\frac{1}{N} \left[\sum_{s=1}^N \sum_{k=1}^C 1\{j_s = k\} \log \frac{e^{\theta_k^T O_s}}{\sum_{k=1}^C e^{\theta_k^T O_s}} \right] + \frac{\lambda}{2} \sum_{n=1}^C \sum_{k=1}^V \theta_{nk}^2 \quad (13)$$

The first term indicates the error item, as well as a subsequent term, represents the weight decomposes. $1\{j_s = k\} = 1$ while $j_s = k; 1\{j_s = k\} = 0$ N represents the count of training samples, $j_s \neq k$. j_s represents the actual output in Eq. (13), wherein V indicates the dimension of the feature vector. The learning model obtains the trainable parameter θ_{nk} .

5.2 NN model

The data features, as well as the image, are considered as the input for the NN [9], and in Eq. (14), (15) as well as (16) the network model is ascertained, wherein, hidden neuron requirement is \bar{h} , $U_{\bar{h}}$ represents a number of input neurons, $W_{(Bh)}^{(HI)}$ represents bias weight to \bar{h}^{th} hidden neuron, $W_{(Bj)}^{(OU)}$ represent output bias weight to \bar{j}^{th} layer, U_{hi} represents a number of hidden neurons, $W_{(kh)}^{(HI)}$ represents \bar{k}^{th} input to \bar{h}^{th} hidden neuron $W_{(hj)}^{(OU)}$ represents output weight from \bar{h}^{th} hidden neuron to \bar{j}^{th} layer, as well as NF represents activation function. Eq. (15) indicates the output of the network $\overline{NO_j}$, wherein $|NO_j - \overline{NO_j}|$ represents the error between predicted as well as actual output, NO_j represents actual output.

$$IN^{(HI)} = NF \left(W_{(Bh)}^{(HI)} + \sum_{k=1}^{U_{\bar{h}}} W_{(kh)}^{(HI)} \text{Input features} \right) \quad (14)$$

$$\overline{NO_j} = NF \left(W_{(Bj)}^{(OU)} + \sum_{h=1}^{U_{hi}} W_{(hj)}^{(OU)} IN_{\bar{h}}^{(HI)} \right) \quad (15)$$

$$W^* = \left\{ W_{(Bh)}^{(HI)}, W_{(kh)}^{(HI)}, W_{(Bj)}^{(OU)}, W_{(hj)}^{(OU)} \right\}_{j=1}^{U_{ou}} |NO_j - \overline{NO_j}| \quad (16)$$

Both the classification outcomes such as NN classification as well as CNN classification are integrated to augment the diagnosis accuracy rate. By exploiting the binary OR operation, the classified outcomes are integrated.

To improve the accuracy of the classification, this work tries to identify the best solutions which create better performance. Moreover, the CNN convolutional layer is optimally chosen as well as the features subjected to the NN, in addition, to optimally chosen using the developed model.

5.3 Proposed Optimization Model

The proposed Improved Binary Artificial Fish Swarm Algorithm (IBASFS) optimization model follows top-down optimization which enthuses clustering, searching, chasing, as well as arbitrary behavior of fish in nature to attain the global optimum [10]. It chooses searching behavior by evaluating the consistency of food and the congestion factor within visual distance. In the proposed model, the probabilities r_1 and r_2 are developed in this paper with $0 \leq r_1 \leq r_2 \leq 1$. Eq. (17) denotes the updating model of the swarm.

$$X_i^{g+1} = \begin{cases} X_{r,i}^{g+1}, & 0 \leq r \leq r_1 \\ X_{p,i}^{g+1}, & r_1 \leq r \leq r_2 \\ X_{c,i}^{g+1}, & r_2 \leq r \leq 1 \end{cases} \quad (17)$$

Wherein, $X_{r,i}^{g+1}$, $X_{p,i}^{g+1}$ and $X_{c,i}^{g+1}$ indicates the location of the fish “i” subsequent to the searching, random as well as chasing behavior is carried out. r indicates the random number among 0 to 1.

As eq. (17) is developed on the basis of the real coding, the fish swarm is updated and mapped to discrete space using eq. (18) as well as (19).

$$f(X_i^{g+1}) = \frac{\exp(2 \times |X_i^{g+1}|) - 1}{\exp(2 \times |X_i^{g+1}|) + 1} \quad (18)$$

$$X_i^{g+1} = \begin{cases} 1, & f(X_i^{g+1}) \geq \tau \\ 0, & \text{otherwise} \end{cases} \quad (19)$$

wherein τ indicates random number among 0-1.

Lévy flight indicates an arbitrary walk step that imitates the animal's behavior. It can search arbitrarily as well as alternately with uninterrupted short jumps as well as infrequently large steps that is a

necessary technique to explain the Lévy distribution. It possesses raised population diversity characteristics and enlarging search space, “therefore global optimization capability of method can be enhanced by replacing the original step parameter”. Eq. (20) denotes the Lévy flight step.

$$\begin{cases} \text{Step} = \text{Step}_{\max} \cdot \text{levy}(\cdot) \\ \text{levy}(\cdot) = 0.01 \times \frac{\mu}{|\nu|^{1/\beta}} \end{cases} \quad (20)$$

Wherein, $\text{levy}(\cdot)$ indicates Lévy flight step; Step_{\max} indicates utmost moving step;

$\nu \sim N(0,1)$, $\mu \sim N(0, \sigma_\mu^2)$, and σ_μ is indicated as

$$\sigma_\mu = \left\{ \frac{\Gamma(1+\beta) \sin(\pi\beta/2)}{\Gamma[(1+\beta)/2] 2^{\beta/2}} \right\} \quad (21)$$

wherein; β indicates $(0, 2)$, Γ indicates gamma function.

Using the average of distances from other artificial fish is ascertained and it is stated in eq. (22).

$$\text{AVisual}_i^R = \sum_{\substack{j=1 \\ j \neq i}}^{\text{pop}} D_{i,j}^g (\text{pop} - 1) \quad (22)$$

wherein AVisual_i^R indicates the average visual distance of artificial fish “i”.

6. Result and Discussion

In this section, the experimental analysis of the proposed model with the conventional models was described and it was also explained regarding the thyroid diagnosis technique. Here. The input data and image were given as input. Here, the proposed model was compared with the Artificial Bee Colony (ABC), Particle Swarm Optimization (PSO) [11], Firefly (FF), Genetic Algorithm (GA) [12], and Crow Search (CS) algorithms.

Fig. 2 demonstrates the complete analysis of the proposed model over the existing models. Here, the performance of the proposed model is 13% better than the ABC, 20% better than the PSO, 18% better than the FF, 14% better than the GA, 19% better than the CS in terms of accuracy. Likewise, the overall performance of the proposed model exhibits that superiority over the existing models. Moreover, the proposed model accuracy is better than the conventional models.

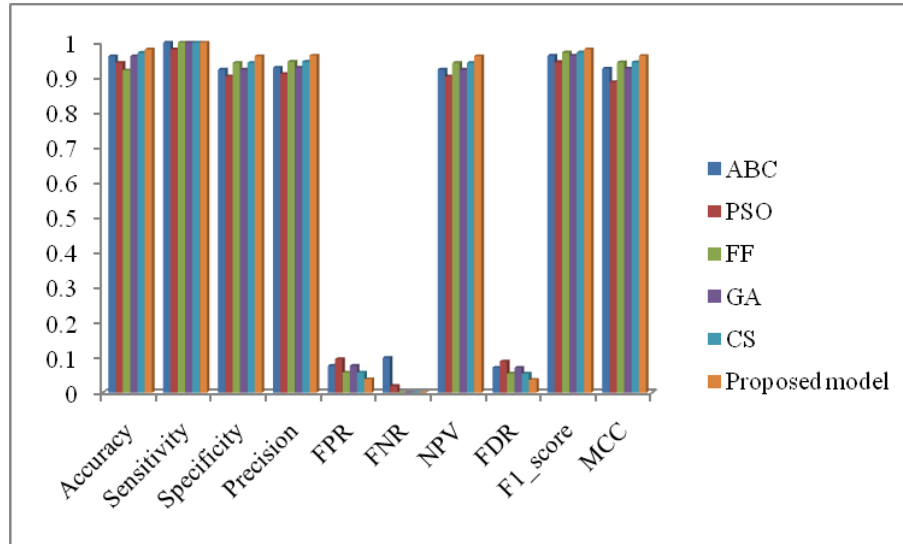


Fig. 2. Performance analysis of the proposed and conventional models

7. Conclusion

The main aim of this work was to propose a novel thyroid detection model, which has incorporated two stages. In the feature extraction process, two sorts of features were extracted. Here, image features such as gradient features as well as neighborhood were extracted. The feature extraction was performed using the PCA from thyroid data. Subsequently, the process of classification was performed in two categories. Here, to obtain the classified outcomes the CNN was exploited bypassing the image. Concurrently, to

perform the classification process, the NN classifier was exploited by obtaining both the data as well as the image features as the input. At last, both the classified outcomes such as NN and CNN were integrated to obtain an accurate diagnosis. The main contribution of this paper was to raise the rate of accuracy, therefore, this research has optimally chosen the CNN convolution layer, as well as the needed features to NN, were chosen optimally. In order to perform this, a novel enhanced approach was presented named IBASFS as well as the performance of the proposed model was with the existing models.

Compliance with Ethical Standards

Conflicts of interest: Authors declared that they have no conflict of interest.

Human participants: The conducted research follows the ethical standards and the authors ensured that they have not conducted any studies with human participants or animals.

Reference

- [1] Yen-Chung Lin, Yi-Chun Lin, Chih-Ching Lin, "Abnormal thyroid function predicts mortality in patients receiving long-term peritoneal dialysis: A case-controlled longitudinal study", *Journal of the Chinese Medical Association*, February 2012.
- [2] I. Tamaskar, R. Bukowski, B. I. Rini, "Thyroid function test abnormalities in patients with metastatic renal cell carcinoma treated with sorafenib", *Annals of Oncology*, February 2008.
- [3] G. Singh, P. Aggarwal, V. Gupta, "Does high serum ferritin predict abnormal thyroid function in transfusion dependent Thalassemia", *Pediatric Hematology Oncology Journal* 30 August 2019.
- [4] Hsin-Hao Chen, Hsiao-Hui Chiu, Shang-Liang Wu, "The Relationship Between Night Shift Work and the Risk of Abnormal Thyroid-Stimulating Hormone: A Hospital-Based Nine-Year Follow-up Retrospective Cohort Study in Taiwan", *Safety and Health at Work* Available online, 1 June 2021.
- [5] E. Sabath, L. Cárdenas-Rodríguez, M. L. Robles-Osorio, "POS-342 HIGH PREVALENCE OF THYROID ABNORMALITIES AND LOW T3 SYNDROME IN MEXICAN SUBJECTS WITH CKD", *Kidney International Reports* 15 April 2021.
- [6] Kuo-Chin Fan and Tsung-Yung Hung, "A Novel Local Pattern Descriptor—Local Vector Pattern in High-Order Derivative Space for Face Recognition", *Ieee Transactions On Image Processing*, vol. 23, no. 7, pp. 2877-89, July 2014.
- [7] Yiping Duan, Fang Liu, Licheng Jiao, Peng Zhao and Lu Zhang, "SAR Image segmentation based on convolutional-wavelet neural network and markov random field", *Pattern Recognition*, vol. 64, pp. 255-267, April 2017.
- [8] Vinay. A, Akshay Kumar C, Gaurav R Shenoy, K.N Balasubramanaya Murthy and S Natarajan, "ORB-PCA based Feature Extraction Technique for Face Recognition", *Second International Symposium on Computer vision and the Internet*, vol. 58, pp. 614-621, 2015.
- [9] Yogeswaran Mohan, Sia Seng Chee, Donica Kan Pei Xin and Lee Poh Foong, "Artificial Neural Network for Classification of Depressive and Normal in EEG", *2016 IEEE EMBS Conference on Biomedical Engineering and Sciences (IECBES)*, 2016.
- [10] Y. Zhu and H. Gao, "Improved Binary Artificial Fish Swarm Algorithm and Fast Constraint Processing for Large Scale Unit Commitment", in *IEEE Access*, vol. 8, pp. 152081-152092, 2020.
- [11] Yogesh R kulkarni, Senthil Murugan T, "Hybrid Weed-Particle Swarm Optimization Algorithm and C-Mixture for Data Publishing", *Multimedia Research*, vol. 2, no. 3, July 2019.
- [12] Raviraj Vishwambhar Darekar, Ashwinikumar Panjabrao Dhande, "Emotion Recognition from Speech Signals Using DCNN with Hybrid GA-GWO Algorithm", *Multimedia Research*, vol. 2, no. 4, October 2019.